Biochemistry and Biophysics Reports 9 (2017) 36–41

Contents lists available at ScienceDirect

Biochemistry and Biophysics Reports

journal homepage: www.elsevier.com/locate/bbrep

nsPEF-induced PIP_2 depletion, PLC activity and actin cytoskeletal cortex remodeling are responsible for post-exposure cellular swelling and blebbing

Gleb P. Tolstykh[a,*], Gary L. Thompson[b], Hope T. Beier[c], Zachary A. Steelman[d], Bennett L. Ibey[e]

[a] General Dynamics Information Technology, JBSA Fort Sam Houston, TX, USA
[b] Oak Ridge Institute for Science & Education, JBSA Fort Sam Houston, TX, USA
[c] Air Force Research Laboratory, 711th Human Performance Wing, Airman Systems Directorate, Bioeffects Division, Optical Radiation Bioeffects Branch, JBSA Fort Sam Houston, TX, USA
[d] Duke University, Durham, NC, USA
[e] Air Force Research Laboratory, 711th Human Performance Wing, Airman Systems Directorate, Bioeffects Division, Radio Frequency Bioeffects Branch, JBSA Fort Sam Houston, TX, USA

ARTICLE INFO

Keywords:
Nanosecond pulsed electric field
Nanopores
PIP_2 hydrolysis
Cellular swelling and blebbing
Calcium

ABSTRACT

Cell swelling and blebbing has been commonly observed following nanosecond pulsed electric field (nsPEF) exposure. The hypothesized origin of these effects is nanoporation of the plasma membrane (PM) followed by transmembrane diffusion of extracellular fluid and disassembly of cortical actin structures. This investigation will provide evidence that shows passive movement of fluid into the cell through nanopores and increase of intracellular osmotic pressure are not solely responsible for this observed phenomena. We demonstrate that phosphatidylinositol-4,5-bisphosphate (PIP_2) depletion and hydrolysis are critical steps in the chain reaction leading to cellular blebbing and swelling. PIP_2 is heavily involved in osmoregulation by modulation of ion channels and also serves as an intracellular membrane anchor to cortical actin and phospholipase C (PLC). Given the rather critical role that PIP_2 depletion appears to play in the response of cells to nsPEF exposure, it remains unclear how its downstream effects and, specifically, ion channel regulation may contribute to cellular swelling, blebbing, and unknown mechanisms of the lasting "permeabilization" of the PM.

1. Introduction

Exposure to nanosecond pulsed electrical fields (nsPEF) results in a myriad of observable cellular effects, including alteration of intracellular Ca^{2+} homeostasis, nuclear granulation, cytoskeletal changes, cellular blebbing, swelling, and initiation of apoptotic cell death [1–8]. While these effects are often attributed to the direct nanoporation of both the plasma and organelle membranes [9–11], the underlying mechanisms are not well understood.

Some of these nsPEF-induced biological effects appear to be similar to situations observed during the normal lifespan of mammalian cells. For example, plasma membrane (PM) blebs occur during cytokinesis, cell migration, proliferation, and apoptosis [12]. It has been shown that both PIP_2 and phosphoinositide-specific PLC are required for regulation of cortical actin dynamics during cytokinesis, since PIP_2 needs to be continuously hydrolyzed for successful completion of cell division, and its hydrolysis pair diacylglycerol (DAG) with protein kinase C (PKC) to stimulate cellular growth and proliferation [13,14]. Likewise, PIP_2 and phosphoinositide-specific PLC are heavily involved in regulation of vital cellular functions such as modulation of PM transport proteins, cytoskeleton dynamics, intracellular Ca^{2+} homeostasis, and regulation of cellular volume [15–21]. While alterations of these functions have all been observed after nsPEF exposures, their relation to the nsPEF-induced PIP_2 signaling pathway is not understood.

Recently, we confirmed that a single 16.2 kV/cm, 600 ns electric pulse initiates an intracellular phosphoinositide PIP_2 signaling cascade similar to one initiated by activation of $G_{q/11}$-coupled receptors, but in cells without such receptors [22]. PIP_2 depletion by nsPEF exposure was demonstrated by direct monitoring of translocation of optical probes of PIP_2 hydrolysis. The nsPEF-induced PIP_2 signaling mirrored the responses following human muscarinic acetylcholine $G_{q/11}$-coupled receptor (hM_1) activation [22,23]. Additionally, the nsPEF-induced increase in intracellular Ca^{2+} is almost identical to the calcium rise observed after purinergic P_2Y_6 $G_{q/11}$-coupled receptor stimulation [24], further suggesting PLC activation and induction of PIP_2 signaling. Initiation of PIP_2 signaling results in production of DAG and inositol-1,4,5-trisphosphate (IP_3) [25], leading to elevation of cytosolic Ca^{2+} from IP_3-sensitive Ca^{2+} stores and DAG – dependent activation of PKC

* Corespondence to: General Dynamics Information Technology, 4141 Petroleum Road, JBSA Fort Sam Houston, TX 78234, USA.
E-mail address: gtolstykh@gmail.com (G.P. Tolstykh).

http://dx.doi.org/10.1016/j.bbrep.2016.11.005
Received 28 June 2016; Received in revised form 11 October 2016; Accepted 8 November 2016
Available online 11 November 2016

[26].

Permeabilization of the PM by nsPEF is an important step in initiation of the response, but cannot be solely accounted for the long-lasting effects due to the theoretically predicted short lifespan (~100 ns) of nanopores in biomembranes [27]. Cell swelling and blebbing occurs seconds after nsPEF exposure and lasts for minutes, comparable to the time needed for PIP_2 recovery back to the PM [22,23]. Since PIP_2 is known to anchor cortical actin [28] and PLC-dependent PIP_2 hydrolysis modulates cytoplasmic cell volume regulatory ion channels [29,30], we hypothesize that nsPEF-stimulated PLC activity and resulting PIP_2 depletion are primarily responsible for the post-exposure, physiological effects of actin cortex remodeling, cellular swelling, and blebbing. This work aims to further expand our previous findings that disintegration of the cortical actin structures is related to cellular swelling initiated by transmembrane diffusion of water after nsPEF-induced PM nanoporation [7].

2. Methods

2.1. Nanosecond pulse exposure

Single and multiple (20 at 5 Hz rate) nsPEFs were delivered to cells using a pair of 125 μm-diameter tungsten electrodes spaced 120 μm apart as detailed in previous publications [1,4,22,23]. Finite difference time domain (FDTD) modeling was used to model the exposure system, and FDTD modeling predicted a 16.2 kV/cm peak field for a 1 kV charging voltage (0.5 kV nsPEF amplitude). To synchronize image acquisition and pulse delivery, a Stanford DG535 digital delay generator was programmed to trigger the Zeiss LSM-710 confocal microscope to begin image acquisition. After a 5-s preset delay, a HP 8112 A pulse generator delivered a specific number of nsPEFs.

2.2. Probe of PIP_2 hydrolysis

PLCδ-PH-EGFP DNA construct (Addgene plasmid 21179) [22,23] was transiently transfected into the Chinese hamster ovarian (CHO) cells already stably expressing m-Apple-actin or G_{q11}-coupled hM_1 and angiotensin II (AngII) receptors using a Lonza 2D Nucleofector™ device. Dr. Mark S. Shapiro (Department of Physiology, University of Texas Health Science Center at San Antonio) kindly provided the hM_1 and AngII cells lines [31], and the m-Apple-actin cell line was created in-house as previously described [7].

2.3. Experimental procedures

The m-Apple-actin, hM_1, and AngII receptor stable cell cultures used a standard complete growth medium consisting of Ham's F-12K media supplemented with 10% fetal bovine serum (FBS), 1% penicillin/streptomycin antibiotic, and 0.48% G418 to ensure transfection stability. Cells were plated on poly-L-lysine coated 35 mm glass coverslip bottom dishes (MatTek No. 0, Ashland, MA) for 24 h prior to experimentation. Cells were rinsed to remove any residual growth medium, and 2 mL of a standard buffer solution (pH 7.4, 290–310 mOsm) that consisted of 2 mM $MgCl_2$, 5 mM KCL, 10 mM HEPES, 10 mM Glucose, 2 mM $CaCl_2$, and 135 mM NaCl was added. In some experiments, the $CaCl_2$ was replaced with 2 mM K-EGTA to create Ca^{2+}- free external buffer.

For intracellular Ca^{2+} measurement, CHO-hM_1 cells were loaded with Calcium Green-1 AM ester (CaGr). A 2 μL aliquot of 3 mM CaGr stock was added to 2 mL of standard buffer, and administered to cells incubated at 37 °C for 30 min. After 30 min, the loading buffer was replaced with standard buffer and images were collected using an inverted Zeiss 710 LSM confocal microscope equipped with a 40X (1.3 N.A.) oil immersion objective.

To compare nsPEF effects with well-known effects caused by endogenous PLC activation, some experiments were paired with $G_{q/11}$-coupled hM1 receptor agonist oxotremorine (OxoM, 10 μM) or AngII receptor agonist angiotensin II (AngII, 10 μM). In a subset of experiments, cells were incubated with PLC blocker edelfosine (10–20 μM) for 30 min prior to OxoM, AngII, or nsPEF exposure. Agonists were added by circulating fresh bath buffer containing either OxoM or AngII at a flow rate of 2 mL/min. All media, chemicals and pharmaceuticals were obtained from Life Technologies, Tocris Bioscience or Sigma-Aldrich. Also, 4 mM propidium iodide (PI) (BD Bioscience) was added to the external solution during some experiments to verify cell viability.

2.4. Data analysis

Cell fluorescence was measured using ImageJ software (NIH) [32]. To measure CaGr fluorescence changes, regions of interest (ROI) were drawn in the cytoplasmic region of cells under study. For PLCδ-PH-EGFP and m-Apple-actin fluorescence measurements, ROI were carefully drawn to demark the PM and the cytoplasm of the cell. We used slightly wider ROI during PM measurements to compensate for PM moving during blebbing. Mean fluorescence was measured for each ROI for all images using ImageJ Multi-Measure. Similarly, to measure cell perimeter lengths, ROI were hand-drawn around each cell, and the perimeter was measured. These values were transferred to GraphPad Prism 6 software for statistical analysis and plotting. The responses were calculated for each cell as a percentage difference (ΔF, %) from the mean of the four frames prior to exposure (Baseline) to the frames taken after exposure (Value) using the formula: 100×(Value – Baseline)/Baseline. All imaging experiments were performed at one frame per second (1 Hz).

3. Results and discussion

The roles of local cytoskeleton and changes of intracellular hydrostatic pressure in blebbing cells after nsPEF exposure [7] have been studied previously. However, the role that PIP_2 depletion and hydrolysis play in the nsPEF-induced cellular response has not been evaluated. To achieve this goal, we used edelfosine (ET-18-O-CH3), a synthetic alkyl-lysophospholipid that blocks PLC to prevent PIP_2 hydrolysis [13,33]. Since edelfosine could arrest cell cycle, inhibit cytokinesis, and initiate apoptosis [13,34–36], we performed a series of experiments to determine its safe operational dose. A small fraction of cells (2%) bathed for 20 min in the 10 μM edelfosine containing buffer experienced PI uptake. However, 100% of the cells had PI uptake after the dose of edelfosine was increased above 30 μM (data not shown). PI uptake is a widely accepted sign of attenuation of cellular viability and PM integrity [37].

To verify the potency of edelfosine as a blocker of PLC activity, we monitored intracellular Ca^{2+} release after $G_{q/11}$-coupled receptor activation. By using Ca^{2+}-chelation in outside buffer, we determined that a 20–30 min pretreatment of cells in 10 μM edelfosine resulted in sufficient decrease of PLC-dependent intracellular Ca^{2+} release from the ER (Fig. 1 (A)). In contrast, but similar to our previous observations [23], addition of 10–20 μM edelfosine was unable to completely prevent intracellular Ca^{2+} spikes after a single 600 ns, 16.2 kV/cm electric pulse (EP) (Fig. 1 (B)). The persistence of the intracellular Ca^{2+} rise suggests that the initial nsPEF-induced PIP_2 depletion is a result of strong, direct mechanical impact on the cellular PM, and not PLC-mediated hydrolysis.

Based on these observations, we chose to use 20 μM of edelfosine to maximally block PLC activity. To outline the critical role of PLC in the cell response to nsPEF, all edelfosine experiments were performed in Ca^{2+} containing external buffer. Fig. 2 shows translocation of the PLCδ-PH-EGFP construct from the PM to the cytoplasm after $G_{q/11}$-coupled receptor stimulation by agonists. This stimulation leads to activation of PLC, which then hydrolyzes PIP_2 to IP_3 and DAG. The PLCδ-PH-EGFP construct, with tagged IP_3, accumulates in the cytoplasm – directly

Fig. 1. *Edelfosine effect on intracellular phosphoinositide signaling cascade.* Edelfosine blocks PLC activity, preventing generation of intracellular IP_3 and intracellular Ca^{2+} release. During hM_1 receptor stimulation (A), 10 μM edelfosine prevented intracellular Ca^{2+} rises in a time-dependent manner. During nsPEF exposure experiments (B), 10–20 μM edelfosine was unable to prevent a Ca^{2+} spike, underlining the initial PLC-independent mechanism. Data are presented as mean of Δ% fluorescence changes with SEM.

demonstrating significant reduction of the PM PIP_2 content (Fig. 2 (A) and (B), after AngII 10 μM and OxoM 10 μM treatment, respectively). This robust PIP_2 hydrolysis process was accompanied by massive cellular blebbing (Fig. 2 (A) and (B) white arrows), providing a link between PIP_2 membrane levels and cell blebbing. Application of 20 μM edelfosine completely blocked the downstream effects of PLC activity, even in the presence of specific $G_{q/11}$-coupled hM_1 receptor agonist OxoM (Fig. 2 (C)). The G_{q11}-dependent PIP_2 hydrolysis caused cellular perimeter changes due to blebbing, but without any PM nanoporation. CHO-AngII cells treated with AngII experienced statistically significant perimeters increase from 62.3 ± 1.9 μm to 70.2 ± 2.4 μm (two-tailed *t*-test, P=0.014, n=23). Similarly the CHO-hM_1 cells treated with OxoM had a perimeter increase from 41.8 ± 1.3 μm to 48.07 ± 1.6 μm (two-tailed *t*-test, P=0.005, n=17). The edelfosine pretreated AngII and hM_1 cells had no blebbing, perimeter decrease, and no significant perimeter increase after agonist application (Fig. 2 (C)).

Similar to G_{q11}-receptors stimulation, single and multiple 16.2 kV/cm nsPEF exposures caused PIP_2 depletion in CHO-hM_1 cells with consequential cell swelling and blebbing. Pretreatment of cells with edelfosine significantly reduced post-exposure cellular perimeter changes and eliminated cell blebbing from a single 16.2 kV/cm pulse. A slight increase of post exposure cellular perimeter was observed after one 16.2 kV/cm EP (from 41.1 ± 1.1 μm to 42.4 ± 1.1 μm, P=0.432), and the increase was more noticeable after twenty 16.2 kV/cm EPs (from 44.9 ± 2.29 μm to 48.7 ± 2.48 μm, P=0.296). The summaries of delta percent (Δ%) changes of cell perimeter are presented in Fig. 2 (D). The Δ% changes were: CHO-hM_1 9.8 ± 3 (n=20); CHO-AngII 11.5 ± 2.5 (n=25); and 5.9 ± 2.3 (n=15), 24.2 ± 2.6 (n=13) for 1 and 20, 600 nsPEFs, respectively. In edelfosine-treated groups Δ% changes were: −3.8 ± 1.4 for CHO-hM_1 (n=12); −0.77 ± 0.99 CHO-AngII (n=16); 1.9 ± 0.6 and 6.9 ± 2.1 for 1 and 20, 600 nsPEFs (n=11 and 6).

Blebbing after G_{q11}-receptor stimulation or nsPEF exposure appears to share similar core mechanisms, as blocking PLC activity with edelfosine was able to prevent blebbing in both G_{q11}-receptor agonists and a single nsPEF pulse case and decrease its occurrence in multiple pulse experiments. This persistence of some blebbing in nsPEF-exposed cells could be related to nsPEF-induced nanoporation of the PM, which leads to slight perimeter increase due to cell swelling, in addition to alterations of PIP_2-dependent cell osmoregulation.

A recent study of fixation-induced cell blebbing demonstrated a correlation between blebbing and PIP_2 levels at the PM. In summary, cell fixation-induced blebbing was reduced in PIP_2-containing cells but occurred in PIP_2-depleted cells. Moreover, lowering of the PIP_2 level at cytoskeleton-attaching membrane sites caused bleb formation at these sites [38]. As we have shown that the PIP_2-depletion response appears to persist in nsPEF-exposed cells even after blocking PLC (Fig. 1 (B)), we investigated the relationship between local PIP_2 depletion and cellular blebbing after nsPEF exposure. Surface plots created on cells

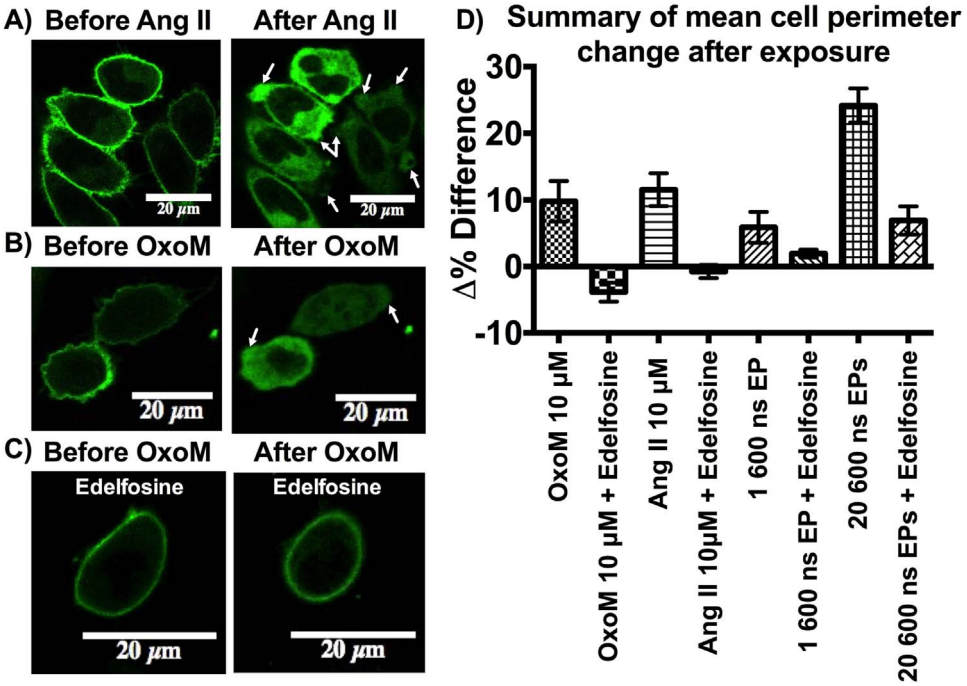

Fig. 2. *PIP_2 depletion and related post-exposure changes in cell perimeter.* Stimulation of G_{q11}-receptors by agonists resulted in PLCδ-PH-EGFP probe translocation from membrane to cytoplasm (signifying PIP_2 hydrolysis) and cellular blebbing with a relative increase of cellular perimeter (A and B). As expected, 20 μM edelfosine prevented such translocation but resulted in a decrease of cellular perimeter (C). A summary of cellular perimeter changes is presented on (D). Data are presented as mean of Δ% fluorescence changes with SEM.

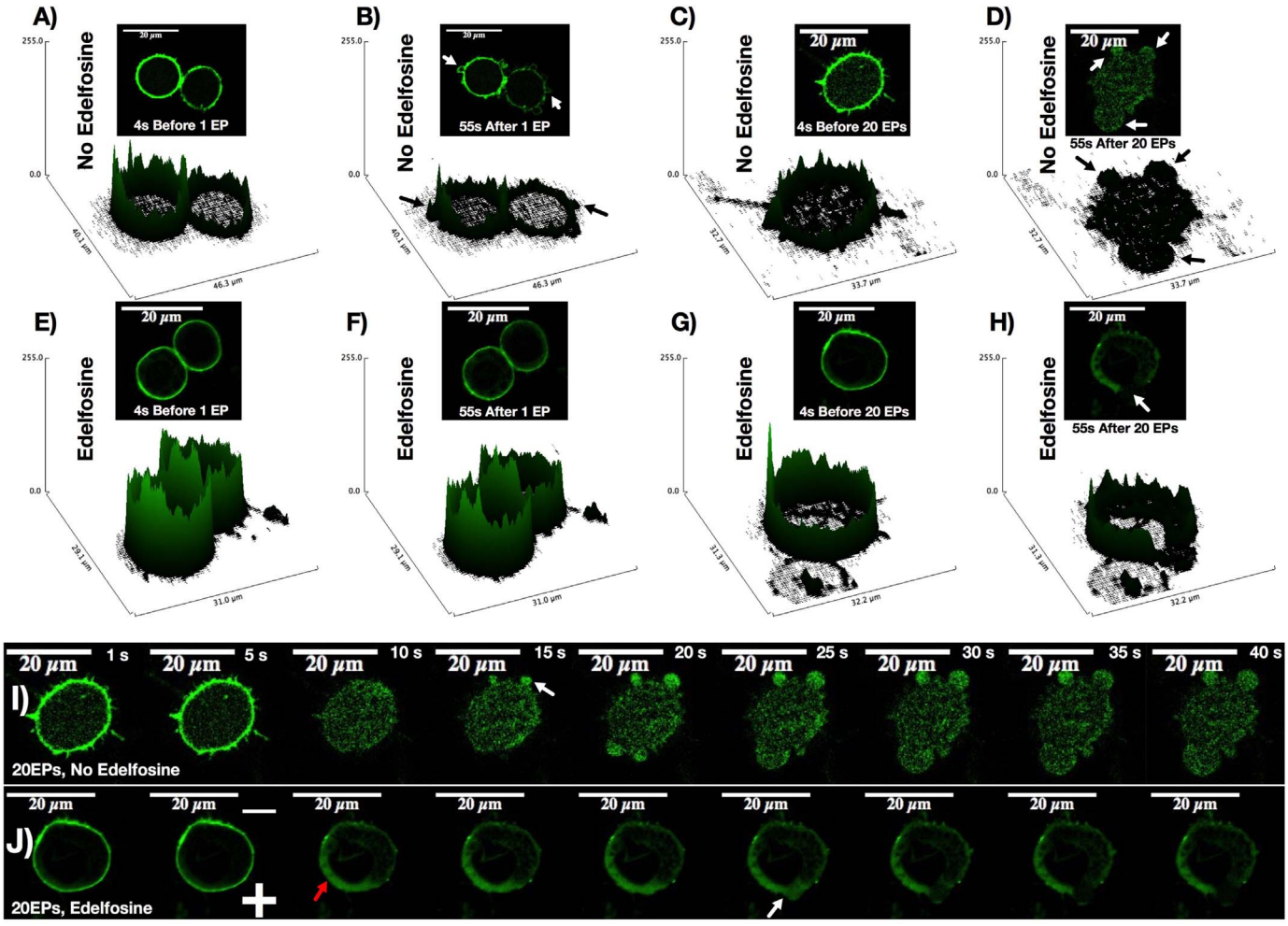

Fig. 3. *Effect of PLC blockage on nsPEF induced PIP_2 cellular effects.* nsPEF exposures resulted in PIP_2 depletion, as tracked by PLCδ-PH-EGFP probe translocation, and cellular blebbing (A, B, C, D). 20 μM edelfosine pretreatment prevented all these effects after a single, 16.2 kV/cm, 600 ns EP (E and F). Twenty pulses resulted in partial PIP_2 depletion on the cell side facing the anodic electrode, with single bleb formation in the same location (G and H). Time lapse of post- 20 pulses of 16.2 kV/cm nsPEF exposure shows cellular effects in normal (I) and edelfosine-treated (J) cells.

before and after single or multiple pulsed EF exposures materialize like a fluorescent ring surrounding the cytoplasm due to strong localization of the PLCδ-PH-EGFP construct to the PM (Fig. 3 (A-H)). Lowering of PIP_2 content after nsPEF-induced PIP_2 depletion resulted in reduction of PM fluorescence due to PLCδ-PH-EGFP translocation to the cytoplasm, as demonstrated by disappearance of the fluorescent ring (Fig. 3 (A) vs. (B) for 1, 16.2 kV/cm 600 nsPEF; (C) vs. (D) for 20, 16.2 kV/cm 600 nsPEFs). Post-exposure cellular blebbing occurred at areas of maximum PIP_2 depletion (Fig. 3 (B) and (D), white and black arrows). Pretreatment of cells with 20 μM edelfosine blocked PLC and prevented PIP_2 depletion, preserving the fluorescent ring in place after exposure (Fig. 3 (E) vs. (F) for 1, 16.2 kV/cm 600 nsPEF; (G) vs. (H) for 20, 16.2 kV/cm 600 nsPEFs). The post-exposure rate of translocation of PLCδ-PH-EGFP from PM to cytoplasm was significantly reduced in edelfosine-treated groups (Fig. 3, (F) vs. (B), and (H) vs. (D)). Note that in the edelfosine-treated group, 20, 16.2 kV/cm 600 nsPEFs caused strong PIP_2 depletion only in the area of the highest field (anode facing), where the bleb formed (Fig. 3 (H), white and black arrows).

The time-course of the PIP_2 depletion and cell blebbing from these multiple pulse exposures are demonstrated in Figs. 3 (I) and 3 (J). Complete PIP_2 depletion was observed after application of 20, 16.2 kV/cm 600 nsPEFs immediately after exposure (Fig. 3 (I), 10 s), and cellular blebbing was observed 10 s after exposure (Fig. 3 (I), 15 s, white arrow). In edelfosine-pretreated cells, a similar exposure to 20 nsEPs produced PIP_2 depletion only on the cell side facing the anodic electrode (Fig. 3 (J), 10 s, red arrow). This observation suggests direct effect of nsPEF exposure on the PM. The underlying mechanism for such a direct effect on the PM remains elusive with possibilities being a stimulus due to mechanical waves or electrophoretic flow, localized reactive oxygen species, or electrodeformation-induced stretch [39–41].

Blebs were formed with a significant time delay of 20 s after exposure (Fig. 3 (J), white arrow), and bleb formation was related to complete local PIP_2 depletion. Thus, cell blebbing after nsPEF impact or G_{q11}-receptors stimulation might be directly related to alteration of the PIP_2 - PM - cortical actin structure. Cortical actin dissociation was linked earlier to blebbing of erythrocytes in patients with chorea-acanthocytosis [42]. In CHO cells, similar observations were reported as a downstream effect of nsPEF exposure [7]. However, the relation between cortical actin disassembly and PM PIP_2 depletion was not demonstrated. To study this relationship, we transiently transfected stable CHO-m-Apple-actin cells with PLCδ-PH-EGFP construct. A 20 16.2 kV/cm 600 nsEPs produced observable PIP_2 depletion 2 s after exposure (green arrows highlight depletion). Conversely, the m-Apple actin distribution is not affected 2 s post exposure (Fig. 4 (A)). According to our previous experiments [23], the peak of PLCδ-PH-EGFP translocation into the cytoplasm occurs within 9 s after exposure. Surprisingly, at 9 s after nsPEF exposure, we noted dimming of the cortical actin fluorescence, and correspondingly, blebbing started in the

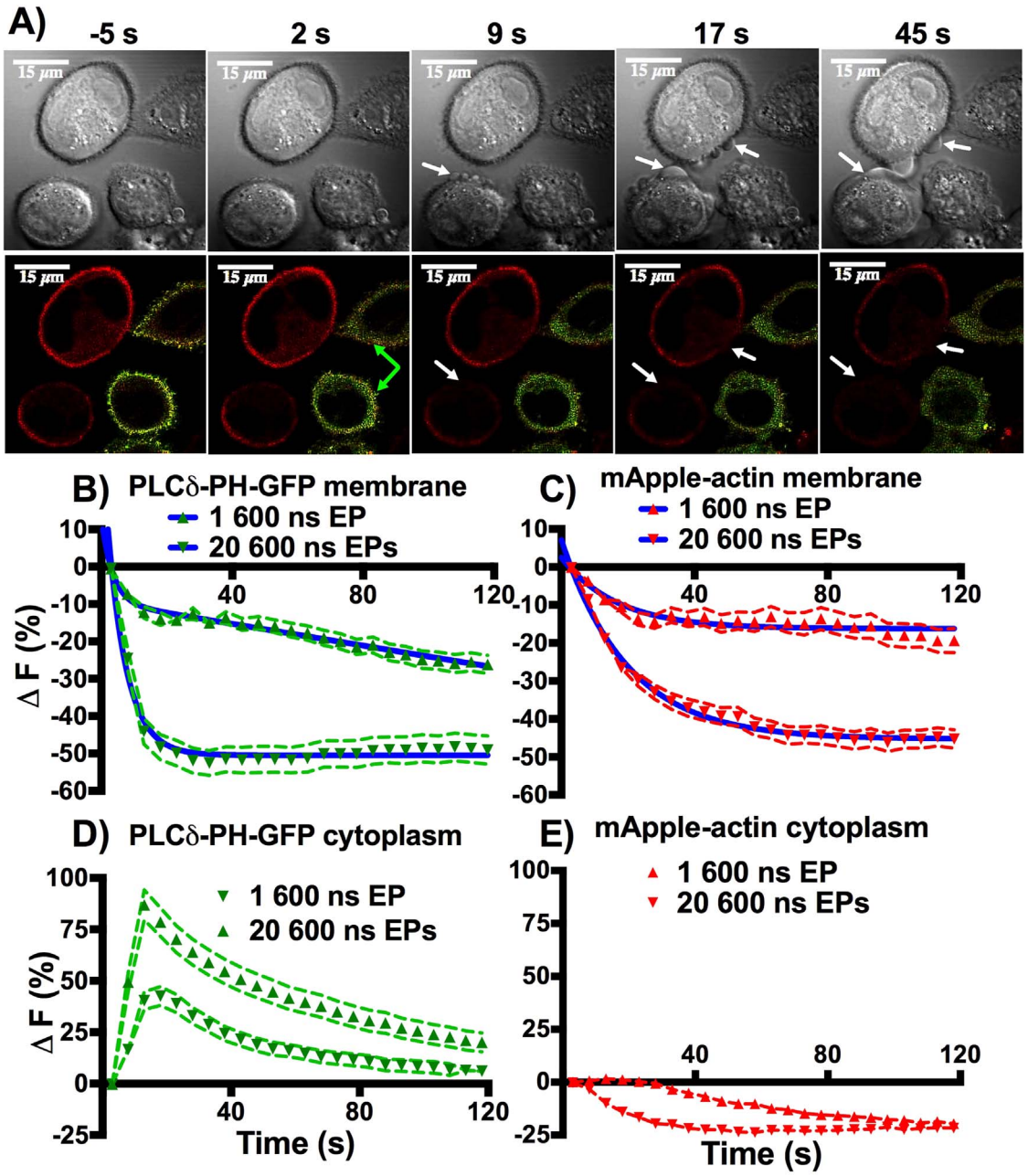

Fig. 4. *Actin cortex and PIP_2 changes after nsPEF exposure.* Actin cortex dissociation is directly related to PIP_2 depletion and cellular blebbing (A). Rapid PLCδ-PH-EGFP probe translocation is observed after nsPEF exposure (B and D). A slower decrease in mApple-actin cortex fluorescence is also observed after nsPEF exposure (C), but without accumulation in the cytoplasm (E). Data are presented as mean of Δ% fluorescence changes with SEM.

same region of the PM (Fig. 4 (A)), at 9 s, white arrows). Thus, actin cortex dissociation follows nsPEF-induced PIP_2 depletion in an EF dose-dependent manner. After nsPEF exposure, PLCδ-PH-EGFP transfected cells show a decrease in PM fluorescence and an increase in cytoplasmic fluorescence (Fig. 4 (B) and (D)). Conversely, only a decrease of PM fluorescence was noted in the mApple-actin group (Fig. 4 (C) and (E)), suggesting actin cortex dissociation and not fluorescent crosstalk from the PLCδ-PH-EGFP emission. Exponential decay analysis revealed a best-fit using two-phase decay (τ_{fast}~6 s for 20 P and ~4 s for 1 P) for PLCδ-PH-EGFP response and one phase decay for m-Apple-actin response (τ~17 s for 20 P and ~11 s for 1 P) (Fig. 4 (B) and (C), blue lines). This finding confirms that actin cortex dissociation follows PIP_2 depletion temporally.

Despite the myriad of reported cell effects after nsPEF (both acute and long term) exposure, we believe that these observations share a root physiological mechanism, namely PIP_2 depletion and PLC activation. This activation is strikingly similar to that observed during G_{q11}-receptor mediated responses to pharmaceutical stimuli. In previous papers, we showed that nsPEF can cause depletion of PIP_2 and activation of PLC in the absence of calcium and that effect appears predominately on the anode portion of the PM [23]. In this paper, we have shown that PIP_2 depletion, PLC activity, and subsequent actin cortex dissociation are the likely origins of the well-documented cellular swelling and blebbing observed after nsPEF exposure. If we accept that PIP_2 depletion and downstream consequences of this depletion occur during nsPEF stimulation, then the role of ion channels and intracellular enzymes in the response of cells to nsPEF cannot be ignored. Furthermore, longer-term consequences such as sensitization, stimulation, and cell death are also related directly to PIP_2 depletion. From this work and previous papers, it is clear that nsPEF-induced

biophysical response is both a physical interaction between the field and the membranes of cells and a resultant biological/biochemical reaction occurring in specific cellular initiated pathways. What remains unclear is the biophysical mechanism(s) underlying nanoporation and depletion of PIP_2 and their further interrelations on the molecular level. Such understanding will be the focus of future work.

Acknowledgments

This work was supported by the Air Force Office of Scientific Research LRIR #13RH08COR. We would like to thank Dr. Mark S. Shapiro for providing CHO cell lines and Ms. Melissa Tarango for technical assistance during our experiments.

Appendix A. Transparency document

Supplementary data associated with this article can be found in the online version at http://dx.doi.org/10.1016/j.bbrep.2016.11.005.

References

[1] C.C. Roth, G.P. Tolstykh, J.A. Payne, et al., Nanosecond pulsed electric field thresholds for nanopore formation in neural cells, J. Biomed. Opt. 18 (2013) 035005..
[2] G.L. Craviso, P. Chatterjee, G. Maalouf, et al., Nanosecond electric pulse-induced increase in intracellular calcium in adrenal chromaffin cells triggers calcium-dependent catecholamine release, Dielectrics and Electrical Insulation, IEEE Trans. on 16 (2009) 1294–1301..
[3] H.T. Beier, C.C. Roth, G.P. Tolstykh, et al., Resolving the spatial kinetics of electric pulse-induced ion release, Biochem Biophys. Res Commun. 423 (2012) 863–866..
[4] G.L. Thompson, C. Roth, G. Tolstykh, et al., Disruption of the actin cortex contributes to susceptibility of mammalian cells to nanosecond pulsed electric fields, Bioelectromagnetics 35 (2014) 262–272..
[5] S.J. Beebe, P.F. Blackmore, J.A. White, et al., Nanosecond pulsed electric fields modulate cell function through intracellular signal transduction mechanisms, Physiol. Meas. 25 (2004) 1077–1093.
[6] S.J. Beebe, P.M. Fox, L.J. Rec, et al., Nanosecond, high-intensity pulsed electric fields induce apoptosis in human cells, FASEB J. 17 (2003) 1493–1495..
[7] A.G. Pakhomov, S. Xiao, O.N. Pakhomova, et al., Disassembly of actin structures by nanosecond pulsed electric field is a downstream effect of cell swelling, Bioelectrochemistry 100 (2014) 88–95.
[8] M.A. Rassokhin, A.G. Pakhomov, Cellular regulation of extension and retraction of pseudopod-like blebs produced by nanosecond pulsed electric field (nsPEF), Cell Biochem Biophys. 69 (2014) 555–566.
[9] A.G. Pakhomov, J.F. Kolb, J.A. White, et al., Long-lasting plasma membrane permeabilization in mammalian cells by nanosecond pulsed electric field (nsPEF), Bioelectromagnetics 28 (2007) 655–663.
[10] O.M. Nesin, O.N. Pakhomova, S. Xiao, et al., Manipulation of cell volume and membrane pore comparison following single cell permeabilization with 60- and 600 ns electric pulses, Biochim Biophys. Acta 2011 (1808) 792–801.
[11] L. Chopinet, M.-P. Rols, Nanosecond electric pulses: a mini-review of the present state of the art, Bioelectrochemistry (2014).
[12] G. Charras, E. Paluch, Blebs lead the way: how to migrate without lamellipodia, Nat. Rev. Mol. Cell Biol. (9) (2008) 730–736.
[13] R. Wong, L. Fabian, A. Forer, et al., Phospholipase C and myosin light chain kinase inhibition define a common step in actin regulation during cytokinesis, BMC Cell Biol. 8 (2007) 15..
[14] M. Serova, A. Ghoul, K.A. Benhadji, et al., Preclinical and clinical development of novel agents that target the protein kinase C family, Semin Oncol. 33 (2006) 466–478..
[15] N. Gamper, Osmosensitivity through the PIP2 availability: just add water, J. Physiol. 588 (2010) 3631–3632..
[16] N. Gamper, V. Reznikov, Y. Yamada, et al., Phosphatidylinositol 4,5-bisphosphate signals underlie receptor-specific Gq/11-mediated modulation of N-type Ca2+ channels, J. Neurosci. 24 (2004) 10980–10992.
[17] N. Gamper, M.S. Shapiro, Regulation of ion transport proteins by membrane phosphoinositides, Nat. Rev. Neurosci. 8 (2007) 921–934.
[18] M.J. Berridge, Inositol trisphosphate and calcium signalling mechanisms, Biochim Biophys. Acta 2009 (1793) 933–940.
[19] D. Raucher, T. Stauffer, W. Chen, et al., Phosphatidylinositol 4,5-bisphosphate functions as a second m essenger that regulates cytoskeleton-plasma membrane adhesion, Cell 100 (2000) 221–228..
[20] S.G. Rhee, Regulation of phosphoinositide-specific phospholipase C, Annu Rev. Biochem 70 (2001) 281–312.
[21] S.G. Rhee, Y.S. Bae, Regulation of phosphoinositide-specific phospholipase C isozymes, J. Biol. Chem. 272 (1997) 15045–15048.
[22] G.P. Tolstykh, H.T. Beier, C.C. Roth, et al., Activation of intracellular phosphoinositide signaling after a single 600 ns electric pulse, Bioelectrochemistry 94C (2013) 23–29.
[23] G.P. Tolstykh, H.T. Beier, C.C. Roth, et al., 600ns pulse electric field-induced phosphatidylinositol-bisphosphate depletion, Bioelectrochemistry (2014).
[24] J.A. White, P.F. Blackmore, K.H. Schoenbach, et al., Stimulation of capacitative calcium entry in HL-60 cells by nanosecond pulsed electric fields, J. Biol. Chem. 279 (2004) 22964–22972..
[25] S.B. Lee, S.G. Rhee, Significance of PIP2 hydrolysis and regulation of phospholipase C isozymes, Curr. Opin. Cell Biol. 7 (1995) 183–189.
[26] E. Oancea, T. Meyer, Protein kinase C as a molecular machine for decoding calcium and diacylglycerol signals, Cell 95 (1998) 307–318.
[27] Z.A. Levine, P.T. Vernier, Life cycle of an electropore: field-dependent and field-independent steps in pore creation and annihilation, J. Membr. Biol. 236 (2010) 27–36..
[28] S.P. Denker, D.L. Barber, Ion transport proteins anchor and regulate the cytoskeleton, Curr. Opin. Cell Biol. 14 (2002) 214–220..
[29] J. Piron, F.S. Choveau, M.Y. Amarouch, et al., KCNE1-KCNQ1 osmoregulation by interaction of phosphatidylinositol-4,5-bisphosphate with Mg2+ and polyamines, J. Physiol. 588 (2010) 3471–3483.
[30] F. Lang, M. Foller, K. Lang, et al., Cell volume regulatory ion channels in cell proliferation and cell death, Methods Enzym. 428 (2007) 209–225.
[31] N. Gamper, J.D. Stockand, M.S. Shapiro, The use of Chinese hamster ovary (CHO) cells in the study of ion channels, J. Pharm. Toxicol. Methods 51 (2005) 177–185..
[32] W.S.Rasband, ImageJ, http://rsbweb. nih. gov/ij/, 2008.
[33] L.F. Horowitz, W. Hirdes, B.-C. Suh, et al., Phospholipase C in living cells activation, inhibition, Ca2+ requirement, and Regulation of M current, J. Gen. Physiol. 126 (2005) 243–262.
[34] A. Ausili, A. Torrecillas, F.J. Aranda, et al., Edelfosine is incorporated into rafts and alters their organization, The journal of physical chemistry, B 112 (2008) 11643–11654..
[35] C. Gajate, F. Mollinedo, Edelfosine and perifosine induce selective apoptosis in multiple myeloma by recruitment of death receptors and downstream signaling molecules into lipid rafts, Blood 109 (2007) 711–719..
[36] F. Mollinedo, C. Gajate, S. Martin-Santamaria, et al., ET-18-OCH3 (edelfosine): a selective antitumour lipid targeting apoptosis through intracellular activation of Fas/CD95 death receptor, Curr. Med Chem. 11 (2004) 3163–3184..
[37] Y. Yang, Y. Xiang, M. Xu, From red to green: the propidium iodide-permeable membrane of Shewanella decolorationis S12 is repairable, Sci. Rep. 5 (2015) 18583..
[38] S. Zhao, H. Liao, M. Ao, et al., Fixation-induced cell blebbing on spread cells inversely correlates with phosphatidylinositol 4,5-bisphosphate level in the plasma membrane, FEBS Open Bio 4 (2014) 190–199..
[39] C.C. Roth, R.A. Barnes, B.L. Ibey, et al., Cells exposed to nanosecond electrical pulses exhibit biomarkers of mechanical stress, 2015, pp. 932612–932612–932618.
[40] C.C. Roth, S. Maswadi, B.L. Ibey, et al., Characterization of acoustic shockwaves generated by exposure to nanosecond electrical pulses, 2014, pp. 89411O–89411O–89410.
[41] O.N. Pakhomova, V.A. Khorokhorina, A.M. Bowman, et al., Oxidative effects of nanosecond pulsed electric field exposure in cells and cell-free media, Arch. Biochem Biophys. 527 (2012) 55–64.
[42] M. Foller, A. Hermann, S. Gu, et al., Chorein-sensitive polymerization of cortical actin and suicidal cell death in chorea-acanthocytosis, FASEB J. 26 (2012) 1526–1534.